





Establishment of Subtrochanteric Fracture in Pre-Clinical Animal Model

Poornima Palanisamy¹ | Simon Kwoon-Ho Chow^{2,3} | Shuai Li¹ | Michelle Meng-Chen Li² | Wing-Hoi Cheung² | Ling Qin² | Yong-Ping Zheng^{1,4}

¹Department of Biomedical Engineering, The Hong Kong Polytechnic University, Hong Kong, SAR, China | ²Musculoskeletal Research Laboratory, Department of Orthopaedics and Traumatology, Hong Kong Special Administrative Region, The Chinese University of Hong Kong, Hong Kong, SAR, China | ³Department of Orthopaedic Surgery, Stanford University, Stanford, California, USA | ⁴Research Institute for Smart Ageing, The Hong Kong Polytechnic University, Hong Kong, SAR, China

Correspondence: Yong-Ping Zheng (yongping.zheng@polyu.edu.hk)

Received: 5 March 2025 | Revised: 11 July 2025 | Accepted: 17 July 2025

Funding: This work was supported by Research Grants Council, University Grants Committee of the Hong Kong Special Administrative Region, China, T13-402/17-N, AoEM-40220.

Keywords: bone repair | fracture healing | osteotomy | rabbit model | subtrochanteric fracture

ABSTRACT

Objective: About 7%–34% of the femur fracture contributes to subtrochanteric fracture, and only very little research is available about these fractures when compared to common hip fractures. Hence, the aim of this study was to develop a clinically relevant and reproducible open fracture model in rabbits at the subtrochanteric region to understand the fracture healing mechanism at this site and to explore treatment effects of biophysical intervention in future studies.

Methods: An open osteotomy was created in 32 adult New Zealand white rabbits at the subtrochanteric region, followed by customized titanium internal fixations. The internal fixator consists of a 3D printed titanium compression plate with cortical screws for locking. The fracture healing was monitored for 6 weeks, and the corresponding radiography, MicroCT, and histomorphometry analysis were performed at regular intervals.

Results: Four rabbits were excluded due to complications (4/32), including bone dislocation one week post-surgery (3/32). Fracture healing progression was observed in radiographic images. MicroCT analysis showed increased callus volume after 42 days. Histomorphometry revealed remodeled bone area with a higher number of osteocyte cells.

Conclusion: The rabbit fracture model of an open femoral osteotomy at the subtrochanteric region has been successfully established, with the facilitation of an internal fixator consisting of a 3D printed titanium compression plate with cortical screws for locking. Applications of this model are being investigated, including different biophysical stimulation methods for accelerating fracture healing.

1 | Introduction

Bone fractures are one of the serious injuries that often require supportive treatment to recover from the incident as early as possible [1, 2]. About 5%–10% of the fractures result in delayed or nonunion fractures [3]. However, there are some kinds of fractures that are even more serious by their nature and require

immediate intervention and follow-up. One such common fracture location is the hip bone. The common risk factors for hip fracture cases are sex, age>65 years, risk of fall, less physical activity, trauma, etc. [4, 5]. Likewise, subtrochanteric fractures in younger adults as well as geriatric patients are more challenging and often require surgery. The incidence of subtrochanteric fractures is higher in the elderly population between the age

This is an open access article under the terms of the Creative Commons Attribution-NonCommercial License, which permits use, distribution and reproduction in any medium, provided the original work is properly cited and is not used for commercial purposes.

© 2025 The Author(s). Orthopaedic Surgery published by Tianjin Hospital and John Wiley & Sons Australia, Ltd.

group of 65 and 85 years old [6, 7]. These fractures often occur within 5 cm of the lesser trochanter of the proximal femur [8, 9]. The most commonly followed practice includes surgery with intramedullary nailing and sliding hip screws [10-12]. Although the surgeries in the management of these kinds of fractures are complicated, still there requires an adjunctive treatment to speed up the bone healing process as they have a direct effect on morbidity and mortality [13]. While these injuries are considered an important topic on the clinician's side, there is a lack of animal models to study the management of subtrochanteric fractures. The establishment of animal models plays a crucial role in understanding fracture healing mechanisms and the development of new treatments. By developing standardized animal models, it will be very useful to translate the research findings into clinical applications, thereby developing effective therapies for treatments. While there are more investigations going on common hip fractures like femoral neck fractures, there is only very little research on subtrochanteric fractures. This kind of fracture often results in nonunion/malunion due to the unique biomechanics and stress encountered in this region during the fracture event, thereby affecting the blood supply in this area, which further delays the fracture healing process. By creating fractures at this site, our study allows us to fill the sparsely explored research area by investigating its potential clinical benefits. In this study, we have not followed the traditional fixation method like IM nailing because creating IM nailing in a small animal model is quite complicated surgery as the entry and exit point will affect the stability of the fixation. We have chosen a different fixation approach to construct a subtrochanteric fracture model in rabbits for future investigations of bone healing mechanisms at deeper fracture sites and also for those resulting in nonunion and delayed unions. Moreover, the reproducibility of the animal model is associated with the degree of consistency. Therefore, an effective animal model is necessary to study the diaphyseal fracture healing mechanism and for clinical treatment as well. Rabbits are one of the most commonly used animals in orthopedic research. The mid-diaphyseal bone region of rabbits and humans is reported to be similar in fracture toughness and bone mineral density [14, 15]. The configuration and blood supply are also found to be similar; thus, they are used in hip fracture animal model studies [16]. Open osteotomy is considered an excellent model to study the fracture healing mechanisms of

non-unions, and the fracture location can be standardized with this method [17]. The purpose of this study was to develop a simple, reproducible, and cost-effective model for rabbit femur bone fracture healing using open osteotomy. We have described the following through this study:

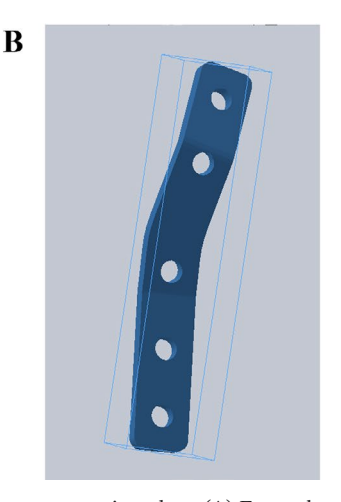
- i. We have created a fresh fracture at the subtrochanteric region of the rabbit femur bone through open osteotomy followed by internal fixation using a customized 3D printed titanium compression plate.
- ii. The fracture healing was evaluated using the outcome measures such as radiography, MicroCT, and histomorphometry after 42 days of fracture.
- iii. Through this study, we have followed a different approach to construct this fracture model and we have achieved a success rate of 87.5% with no side effects to the animals' post-surgery.

2 | Materials and Methods

2.1 | Design and Fabrication of 3D Printed Titanium Internal Fixator

The stabilization of the fractured bone was obtained by implanting suitable fixators at the fracture site as they provide a proper alignment to the bone during the healing process. The use of 3D printing in the fracture management is a promising tool in enhancing the accuracy and efficiency by simulating the surgeries [18]. This technology further allows the design of appropriate fixators for all kinds of bone defect management. In this study, the femur bone from an adult New Zealand white rabbit carcass was harvested and the tissues on the bone surface were removed as shown in Figure 1A. The bone sample was then mounted using a holder inside the MicroCT scanner and prepared for scanning. The optimal resolution for the scanning was set to 2.5 µm. Once the parameter was set, the scanning was done automatically by the machine. The 3D image of the scanned bone was generated by the built-in image reconstruction software of the MicroCT scanner. The reconstructed data was extracted in STL format, and the 3D model of





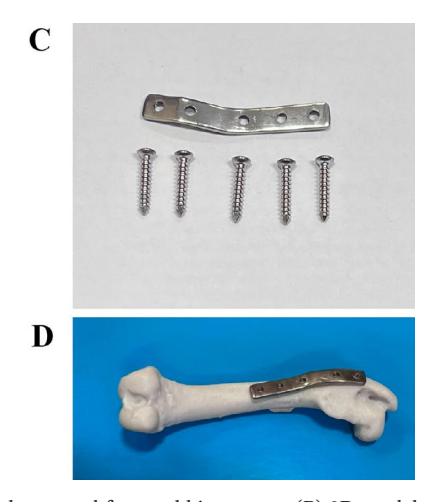


FIGURE 1 | Customization of 3D printed titanium compression plate. (A) Femur bone harvested from rabbit carcass, (B) 3D model of implant design, (C) implant with cortical screws, and (D) location of the titanium implant on bone model.

the bone was created with a 3D printer machine at U3DP, The Hong Kong Polytechnic University.

A customized bone plate was designed using SolidWorks software (Solidworks; Dassault Systèmes Solidworks Corp.) and the model was 3D printed using titanium alloy as shown in Figure 1B,C. Finally, the implant was tested on a 3D bone model to ensure the geometrical fitting over the bone and also to avoid further dislocations after the surgery (Figure 1D). The customized compression plate consisted of five locking screws with a diameter of 1.5 mm for each screw hole and the thickness of the plate was 1.2 mm. The weight of each bone plate was 1g. The fixation screws were purchased from a standard company (BIORTHO CO LTD, Jiangsu, China) producing 'A-grade' veterinary screws specifically for animal surgeries. The outer diameter of these screws was 2 mm, and the length of the screw was 12 mm. All the bone plates and the screws were disinfected ultrasonically in absolute acetone followed by ethanol as a final process.

2.2 | Experimental Animals

All the experimental procedures were conducted after obtaining approval from the Animal Experimentation Ethics Committee of The Chinese University of Hong Kong (Ref no. 20-051-MIS) and the license issued by the Department of Health of the Hong Kong Government. Thirty-two adult New Zealand white rabbits with an average body weight of 1.8 kg (1.6–2 kg) were used in this study. To achieve a statistical power of 0.8, with an effect size of 0.5 in detecting the difference at a significance level of 0.05, the study requires 28 rabbits. By considering the drop rate of about 10%, we have used 32 rabbits. All the rabbits, upon their arrival, were kept in individual metal cages in the central animal facility LASEC Centre at CUHK, and they were supplied with standard

food for the rabbits and water *ad libitum*. The metal cages were kept in a room with a controlled temperature of 19.4°C and 73% humidity that had a 12-h light and dark cycle, with the room lighting kept on from 6 am to 6 pm every day.

2.3 | Surgical Procedures

2.3.1 | Operative Method: Subtrochanteric Fracture

Before starting each surgery, the animals were weighed individually. Under general anesthesia, an intramuscular injection was given by a mixture of ketamine (50 mg/kg) and xylazine (10 mg/ kg). The anesthetic condition of the rabbit was confirmed by the rabbit's eye-lip reflex motion along with a relaxed breathing pattern. All the surgical instruments, implants, and screws underwent autoclave before use. The surgical site was shaved carefully and followed by disinfection of the site using 70% ethanol and prepared for the surgical procedure (Figure 2). The rabbit was then draped in a sterile cloth leaving the surgical site exposed. To create an open osteotomy fracture in rabbits, a skin incision was given by a scalpel blade (surgical blade, size 23). Following the incision, the muscles (biceps femoris muscle and semimembranosus muscle) were retracted (Figure 2B) to find the subtrochanteric region of the femoral bone. An air-powered sagittal oscillating saw (Model no.: 05.001.082, Air pen drive, DePuy Synthes, Germany) with a 1 mm blade thickness was used to create the open osteotomy at the subtrochanteric region. Five holes were created (Figure 2C) with a drilling bit of diameter 1.5 mm, and a thread length of 12 mm was created for screw fixation. After the creation of drill holes, the 3D printed titanium implant was internally fixed using five selftapping cortical screws (Figure 2D) of diameter 2mm. The gap of the osteotomy site was 1 mm. A simple transverse subtrochanteric fracture with no comminution was first verified by direct

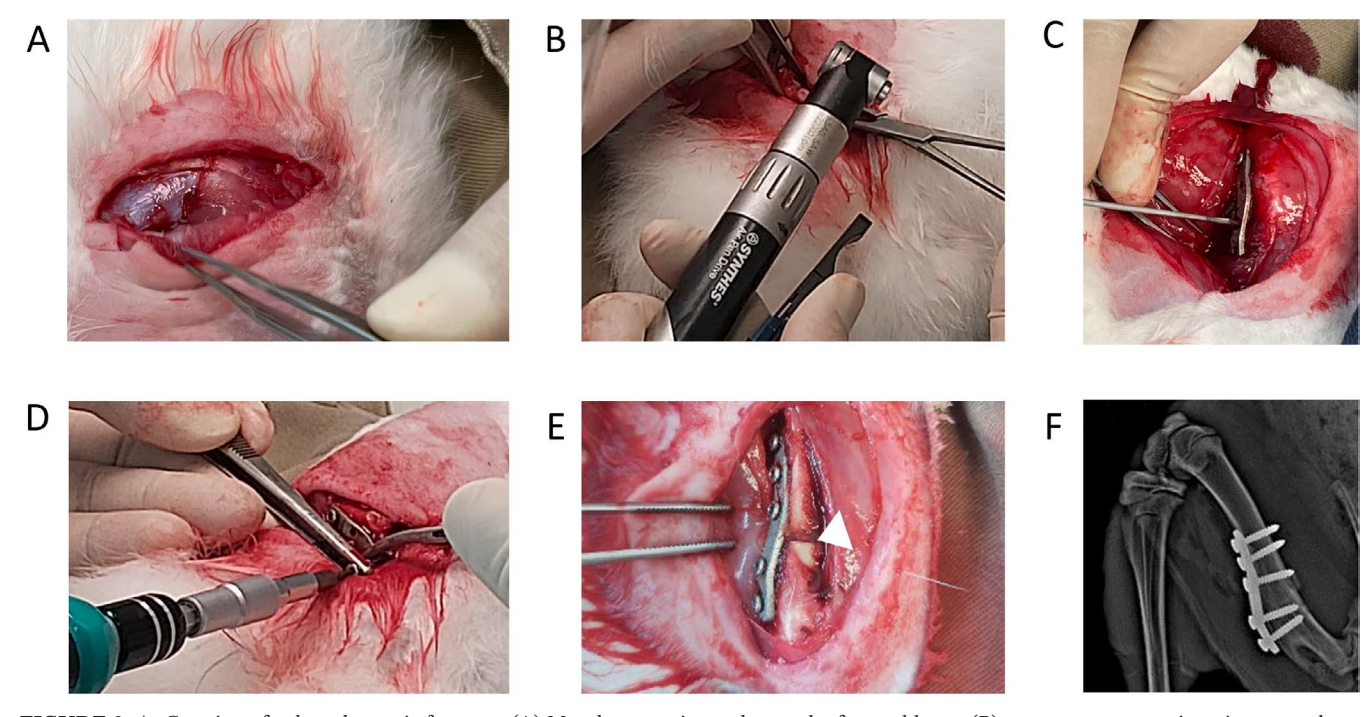


FIGURE 2 | Creation of subtrochanteric fracture. (A) Muscle retraction to locate the femoral bone, (B) open osteotomy using air-powered saw to create the fracture, (C) drill bit used to create holes for screw fixation, (D) fixation of self-cortical screws, (E) the arrow denotes the fracture line created, and (F) post-surgical radiography.

2728 Orthopaedic Surgery, 2025

visualization (Figure 2E). The surgical site was cleaned using sterile saline. Finally, the connective tissue layers were closed with non-absorbable 8–0 nylon sutures, and the skin was closed with 4–0 nylon sutures (MERSILK, W580, ETHICON, USA). The overall surgical procedure took 20 min per rabbit. A post-operative radiograph was taken immediately after the suturing to confirm the successful fracture and implant fixation (Figure 2F). Post-surgery, an intramuscular injection of 0.1 mL of buprenorphine (analgesia) was administered twice a day up to three consecutive days. The animals were given post-surgical care for their speedy recovery. After the surgery, the animals were allowed to move freely inside the cage. From the second day after the surgery, the animals were found active inside the cage. The physiological condition of the rabbits was monitored regularly to ensure the occurrence of any post-surgical complications.

2.4 | Clinical Monitoring

The welfare of the animals was observed by monitoring the parameters such as body weight, general clinical signs, pain signs through behavior, surgical site, and post-operative support.

2.5 | Radiography

A right lateral recumbent view of the femoral bones was taken immediately by an X-ray machine (KUBTEC XPERT-80, Stratford, USA) after the operation by placing the rabbit's fracture limb in the center of the field of vision. X-rays were taken to confirm that the implant fixation is retained in the trochanteric region and the fracture ends were fixed, so as to prove the success of the rabbit fracture model construction. The osteotomy line was identified to separate the newly formed bone. At the same time, weekly radiographs were checked to monitor the fracture healing.

2.6 | MicroCT Analysis of New Bone Formation

All the rabbits were euthanized after 6 weeks of monitoring and the femoral bones were harvested. The soft tissues around the bones were dissected carefully and the titanium implants along with the screws were removed carefully without causing disturbance to the fracture site. The scanning was performed by a multi-slice peripheral quantitative computed tomography-pQCT (xtremeCT, Scanco Medical, Bruttisellen, Switzerland) [19]. The region of interest within the fracture area was evaluated by the inbuilt software of XtremeCT. The bones were kept in a plastic tube and placed inside the scanning holder using adhesive tape. An X-ray source of 60 kVp with an effective dose less than 5 μSv was performed on a segment of 6.5 mm starting from 3 mm proximal to the fracture line. A total of 80 CT slices with a nominal resolution of 82 µm were reconstructed into a three-dimensional (3D) image. The callus volume (mm³) near the fracture region and the corresponding contralateral side was measured.

2.7 | Histomorphometry

After the mechanical testing, the femoral bones were fixed in 10% neutral buffered formalin for 48h and decalcified in 10%

formic for 8 weeks to undergo the dehydration process. The bones were cut into two halves along the midsagittal plane, embedded in paraffin wax, and sectioned at $7\mu m$ thick longitudinally up to five sections in the sagittal plane using a microtome blade and stained in hematoxylin and eosin. A light microscope system (Leica, DMRB DAS, Leica, Heerburgg, Switzerland) was used to analyze the cellular components found in the fracture site [20]. The region of interest was evaluated within the stained area.

2.8 | Data Analysis

The statistical analyses were performed using GraphPad Prism (GraphPad Software Inc., LaJolla, CA, USA). Representative images for radiography, MicroCT, and histomorphometry depict the fracture creation and callus formation at the region of interest. Continuous variables such as callus volume were summarized in terms of mean and standard deviation. For normally distributed data, an independent Student t-test was performed. The p-value is set to <0.05, which denotes the statistical significance of the results.

3 | Results

3.1 | Failure Parameters for Euthanasia/Exclusion From the Study

The average age of rabbits used in this study was 11 weeks old. Four rabbits encountered complications that required euthanasia/exclusion from the analysis (Table 1). One rabbit was excluded from the experiment since the implant got displaced away from the bone, the very next day after the surgery. Three other rabbits were excluded from the study after the displacement of the implant as well as the bone that occurred in their first post-operative week. No other animal showed any kind of complications or infections throughout the experimental period.

3.2 | Radiographical Evaluation of the Fracture

Fracture gap was visible from week 1 till week 2. Figure 3 shows the radiographic progression indicating the visible callus formation in the diaphyseal region from week 3 to week 6 post-fracture.

TABLE 1 | Summary of success and failure cases post-surgery (total n = 32).

	Success cases	Failure o	cases
		Implant displacement	Bone displaced one-week post- surgery
No. of animals	28	1	3
Percentage (%)	87.5	3.1	9.3

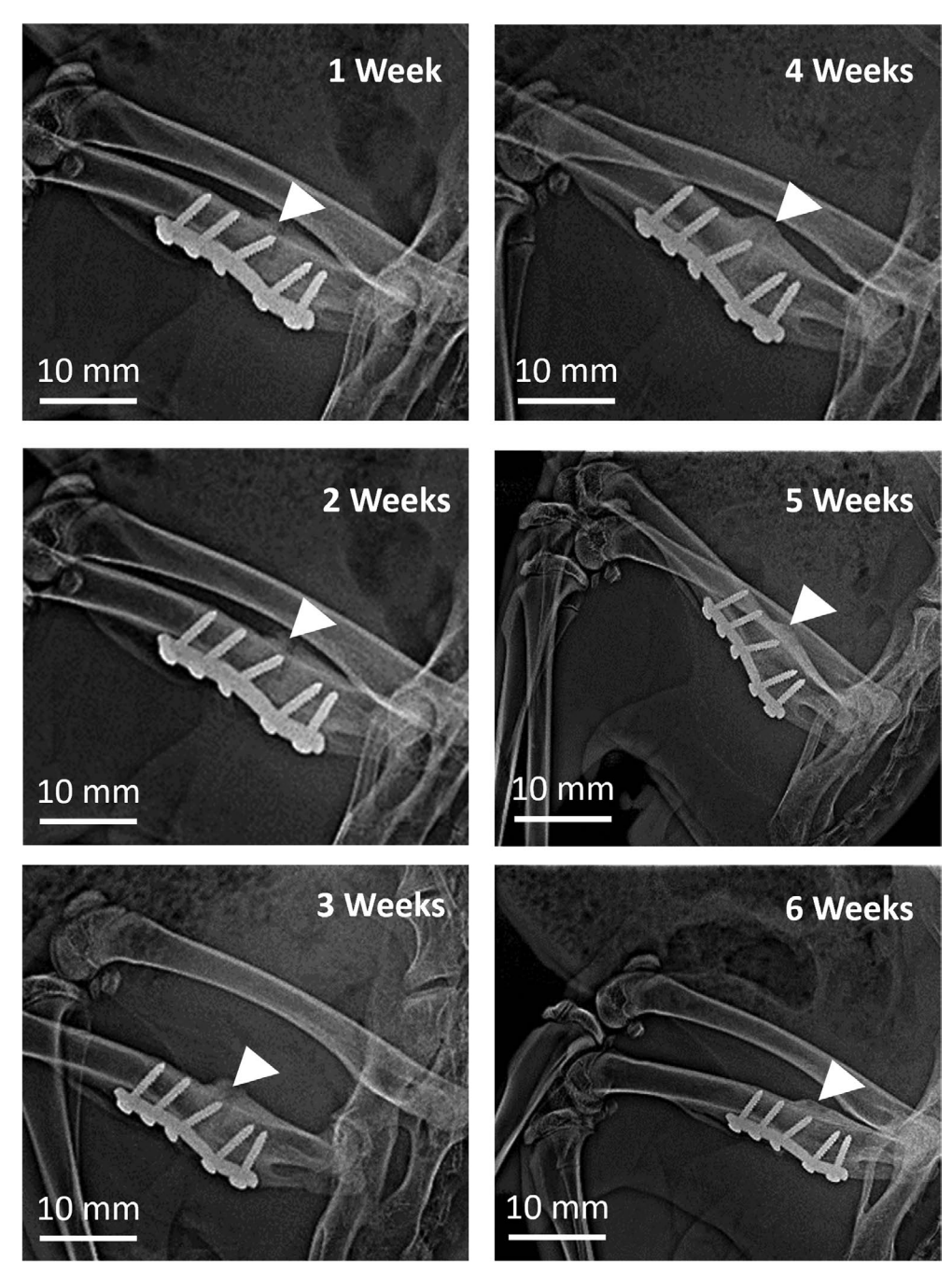


FIGURE 3 | Radiographs of rabbit's left femoral bone at different weeks post fracture. The arrow in the X-ray shows bone union stages during fracture healing.

The fracture gap was completely consolidated in all of the rabbits 42 days post-fracture. A continuous progression of consolidation of the fracture gap was observed till the completion of the experimental period. Since the fracture at the diaphyseal region would not have significant callus formation, we did not measure the callus formation width in this study. The bone union was achieved with an average consolidation time of 4.2 months.

3.3 | Clinical Behavior of the Rabbits

Starting from the surgery day, each rabbit was weighed every week (Table 2). After 1 week of post-surgery, there was a slight reduction in body weight (~100g) in very few rabbits when

compared with the weight measured before the surgery. After the second week, all rabbits showed a significant improvement in weight gain, which was normal according to their growth, and reached their maximum weight of 2.8 kg by the end of week 6. The rabbits were monitored regularly from day 1 of surgery. During the first week of the surgery, the activity level of the rabbits was less inside the cage. Post-surgery 1 week, the animals started to show full weight bearing on all four limbs. From week 2 onwards, all the rabbits went back to their normal lifestyle of being active inside the cage. One rabbit was found to be stressful, which was noticed by biting its own feet. Hence supportive care was given by administering a painkiller for additional 4 more days, and the wound was disinfected by povidone-iodine (Betadine, Mundipharma, Switzerland) followed by 70%

		Average body weight 6 weeks	Difference in body weight	Mean percentage change of
No. of animals	Average body weight before surgery (kg)	post-surgery (kg)	before and after surgery (kg)	body weight after surgery (%)
28	1.87 ± 0.29	2.58 ± 0.23	0.71 ± 0.21	39.8 ± 15.7

 TABLE 2
 Change in body weight before and after experimental period.

ethanol. The bitten foot was then wrapped with a self-adhesive bandage (Nexcare 3M, Hong Kong, China) to prevent the rabbit from further biting the foot.

Throughout the study, all the rabbits survived without any complications such as necrosis, wound, or soft tissue damage at the fracture site.

3.4 | MicroCT Quantification of New Bone

The fracture healing outcome was visualized and quantified by MicroCT of dissected femur bone. The 3D reconstructed bone images in cross-section and longitudinal view taken post 6 weeks are shown in Figure 4. The region of interest is indicated by dotted lines. A visibly remodeled bone was noticed within the region of analysis. The callus volume was found to be higher in the fractured side compared to the original bone volume of the unfractured side. However, no significant difference (p = 0.0531) in callus volume (mm³) was observed on the unfractured side. This is due to post 6 weeks of surgery; the fractured side of the rabbit is in the remodeling stage of the healing process.

3.5 | Bone Histomorphometry

Bone remodeling has been confirmed in bone histomorphometry. The representative histology sections show hematoxylin and eosin staining of bone tissue in Figure 5. The diaphyseal region of the bone consists of cortical bone, which is covered by the medullary cavity containing bone marrow. Figure 5B exhibited the presence of an increased area of trabecular bone. A significant number of osteocyte cells, that is, mature bone cells, were found within lacunae at the fracture site. During the fracture healing process, the matured osteoblast cells get embedded into the bone matrix and become osteocytes. Since the bone had undergone complete remodeling, no osteoclastic cells were noticed.

4 | Discussion

In this study we have created an open osteotomy in the rabbit femur bone [17]. The average length and diameter of the rabbit femur bone are 10 and 2.5 cm, respectively. However, we have demonstrated that it is possible to create a subtrochanteric fracture for the first time in an animal model along with a customized 3D printed internal fixator. Our primary finding exhibits the creation of a simple and easily reproducible subtrochanteric fracture model for future investigations of non-unions and delayed union of deeper fracture sites. The regular radiographs taken post fracture have shown continuous successful progression of bone union. The findings of MicroCT images revealed the increased volume of callus formation at the fractured side. Further, the histology staining results also demonstrated the remodeling of bone by the presence of a significant number of mature bone cells (osteocytes) at the osteotomy site. This technique produced consistent fracture healing outcomes with fewer complications due to implants. None of the animals faced side effects such as skin allergy, skin abrasion, and laceration at the fracture site throughout the experimental period.

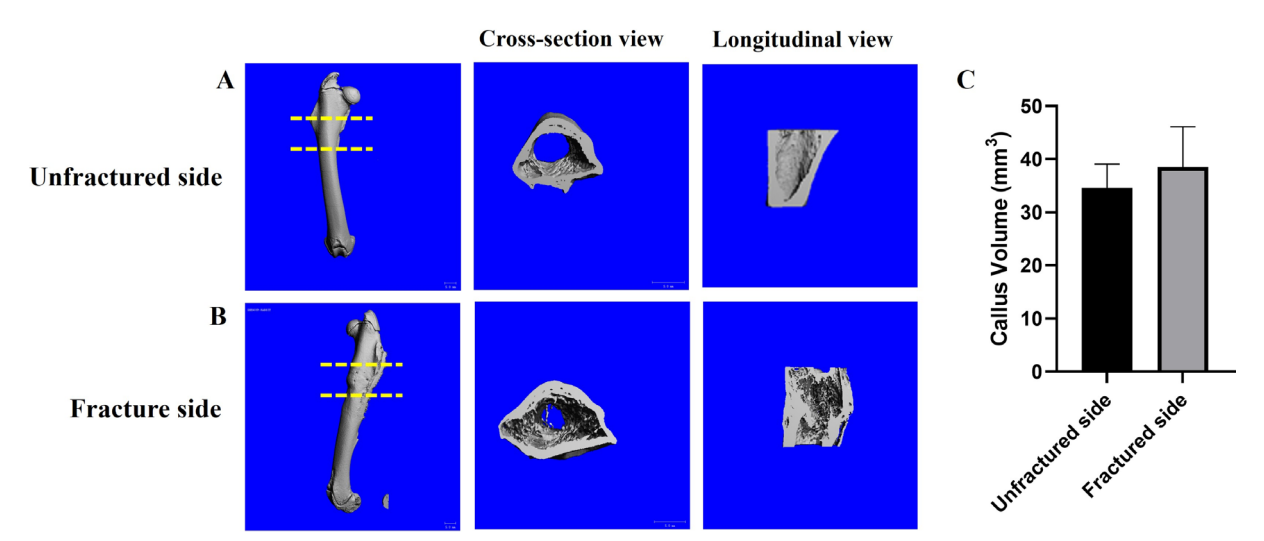


FIGURE 4 | Representative 3D MicroCT images of the newly formed bone after 6 weeks of observation. (A) Unfractured side, (B) fracture side: Yellow dotted lines denote region of analysis, and (C) callus volume measured at the region of analysis. Two-tailed Student's *t*-test was performed between unfractured and fractured side.

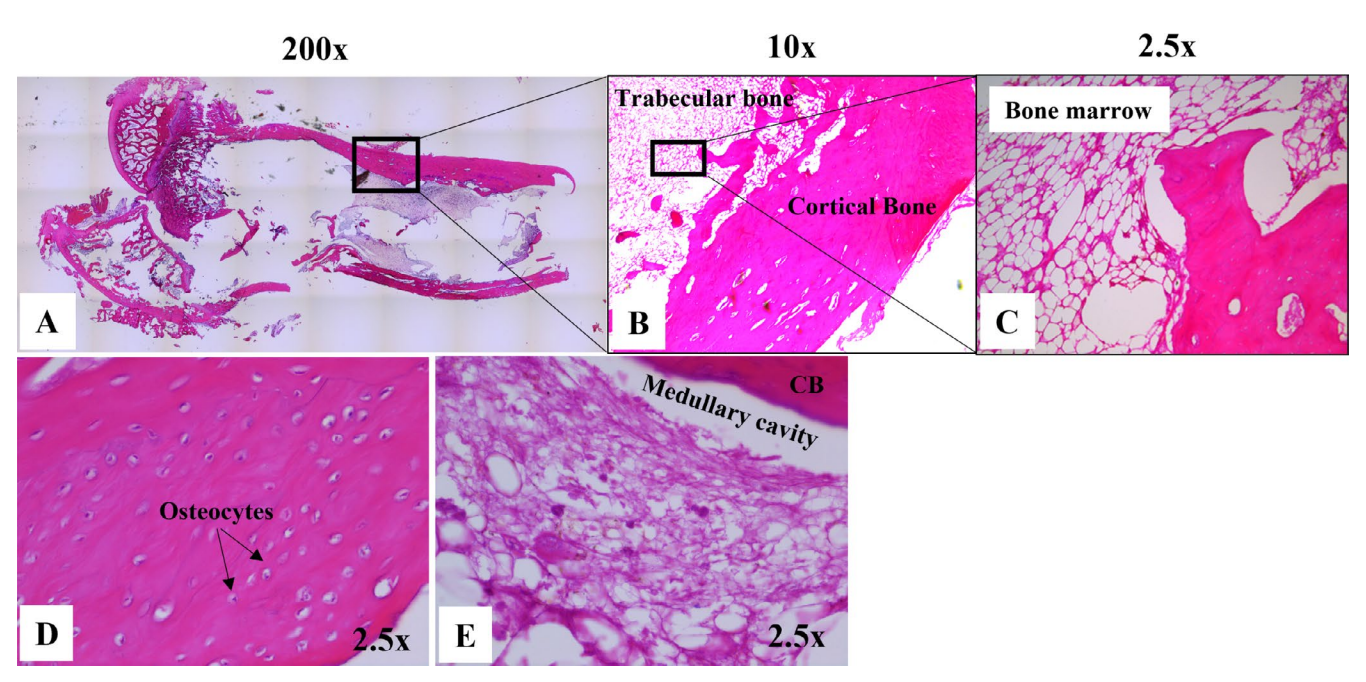


FIGURE 5 | Histological section H&E at 6 weeks post-fracture. (A) Sagittal section of femoral bone stained using hematoxylin and eosin, (B) cortical and trabecular bone images at the fracture site, (C) bone marrow present within the trabecular bone or spongy bone, (D) osteocytes cells found in the cortical bone, osteocytes in lacunae, and (E) medullary cavity is located between cortical bone (CB) and trabecular bone.

4.1 | Radiological Outcome of Subtrochanteric Fracture

A complete bone union is achieved 6 weeks post injury [21]. The phases of bone fracture healing include inflammatory/hematoma phase, followed by angiogenesis, that is, new blood vessel formation [22, 23]. Post angiogenesis, cartilage formation occurs, which leads to calcification of the cartilage. Finally, bone remodeling occurs by gradual removal of cartilage. The present study agreed with these stages of fracture healing. The callus formation was achieved within the first 3 weeks of the fracture event, followed by formation of hard callus and gradual increase of mineralized bone, which resulted in complete bone union.

4.2 | 3D Printed Implants for Animal Models

Osteotomy models are often used to evaluate the mechanical properties of the fixators used. The fracture healing process during osteotomies would purely depend upon the stability of the fixations [24]. In the present study, we have customized a locking plate based on the anatomy of the rabbit femur bone by 3D printing technology. The development of 3D printing technology over the years possesses potential benefits in many biomedical applications due to its mass production and customized fabrication [25]. The implants can be pre-contoured based on the 3D model of the bone, which reduces the complications related to implants. This further helps to improve

2732 Orthopaedic Surgery, 2025

surgical efficiency and accuracy. The current study revealed a success rate of 87.5% using 3D printed implants. We have fabricated the implants using titanium metal. Compared to stainless steel, titanium has greater fatigue resistance and maximum torque [26, 27]. The corrosion properties of the titanium implants are lower, which protects the inside of the body and are good at reducing the toxicity caused by metal debris. Although we have not evaluated the mechanical properties of the implants, none of the rabbits faced delayed or nonunions throughout the observational period.

4.3 | Strengths and Limitations

Our fracture model mimics real fractures mechanically and biologically. The fracture pattern that we have created includes transverse or oblique fracture patterns that commonly occur in humans. Thus, it helps in the assessment of the fracture healing process in real conditions. The radiographic evaluation also found to be similar to that of humans, that is, from the inflammatory phase to the remodeling phase. The implant material used in this study is the same as that in humans which is commonly used, which further enhances mechanical stability and greater flexibility, thus promoting better callus formation. Finally, the time required for fracture healing parallels the stages observed in humans. Altogether, this fracture model provides a great platform for investigating various biophysical interventions and their cellular mechanisms by resembling the real-time fracture scenarios. While this study has successfully provided a novel fracture model to explore the underlying future studies on mechanisms in hip bone fracture healing and their biophysical interventions, there are still some limitations. One limitation of this study is that the fracture healing was not characterized at weekly intervals to understand the bone formation process at each phase of healing at the subtrochanteric region. As the model we have newly established falls into the classification of open reduction internal fixation (ORIF) at a diaphyseal region of a long bone, the healing of bones would follow a typical secondary healing through the process of endochondral ossification. In other words, the evolution of the callus size would be a very good indication of the stage at which the bone has progressed in the healing process [1, 28, 29]. Hence, we have only taken weekly radiographs to monitor the fracture healing progression and implant fixation. Another limitation is that we have not conducted mechanical testing for the unfractured side, leading to the difficulty in assessing the bone strength of the fractured side. In future studies, the bone healing process at different stages can be investigated to understand the fracture healing mechanisms at the inflammatory/hematoma stage and the remodeling stage, and more tests can be conducted to understand more of the healed bone quality.

4.4 | Prospects of Clinical Application

This animal model provides platforms for testing new fixation methods and biophysical interventions that allow research to validate their findings before translation to clinical practices. Further, this model helps in understanding the biomechanical properties of femur bone fracture healing by considering the

load-bearing capacity of the bone. Biological evaluation helps to study the fracture healing mechanism at this region and thereby enhances treatment strategies. We have not encountered any significant problems while creating this fracture model. In the current study, we have used only a reliable sample size. As the study has great clinical significance, a larger sample size should be used in future studies to validate the efficacy of creating this model. As we have used small animal models, the fracture healing mechanism should be tested in larger animal models before translating to humans. The findings from this study can be used in exploring the biophysical interventions at the subtrochanteric region.

5 | Conclusions

We have successfully developed a novel pre-clinical animal model in rabbits for the first time for subtrochanteric fracture healing studies. It is technically a simple model and easily reproducible, thus it can be widely adopted. As closed fracture models are difficult to create at this location and the fracture site cannot be standardized due to the occurrence of comminuted fractures, we have opted for open osteotomy. The fractured bone healed and remodeled within a period of 42 days. This model could be used in future studies to investigate the fracture healing mechanisms at deeper sites, nonunion, and delayed unions, as well as different biophysical stimulation methods.

Author Contributions

Study design (PP, SKHC, LWHC, LQ, YPZ), data collection (PP, SKHC, SL, MMCL), data analysis (PP, SKHC), writing (PP, SKHC, SL, MMCL, LWHC, LQ, YPZ), supervision (LWHC, LQ, YPZ). All authors have read and approved the final submitted manuscript.

Acknowledgments

The authors have nothing to report.

Conflicts of Interest

The authors declare no conflicts of interest.

Data Availability Statement

The data that support the findings of this study are available from the corresponding author upon reasonable request.

References

- 1. T. A. Einhorn and L. C. Gerstenfeld, "Fracture Healing: Mechanisms and Interventions," *Nature Reviews Rheumatology* 11, no. 1 (2015): 45–54.
- 2. P. Palanisamy, M. Alam, S. Li, S. K. Chow, and Y. P. Zheng, "Low-Intensity Pulsed Ultrasound Stimulation for Bone Fractures Healing: A Review," *Journal of Ultrasound in Medicine* 41, no. 3 (2022): 547–563.
- 3. S. Toosi, N. Behravan, and J. Behravan, "Nonunion Fractures, Mesenchymal Stem Cells and Bone Tissue Engineering," *Journal of Biomedical Materials Research Part A* 106, no. 9 (2018): 2552–2562.
- 4. M. Parker and A. Johansen, "Hip Fracture," *BMJ* 333, no. 7557 (2006): 27–30.

- 5. K. E. LeBlanc, H. L. Muncie, Jr., and L. L. LeBlanc, "Hip Fracture: Diagnosis, Treatment, and Secondary Prevention," *American Family Physician* 89, no. 12 (2014): 945–951.
- 6. M. Soveid, A. R. Serati, and M. Masoompoor, "Incidence of Hip Fracture in Shiraz, Iran," *Osteoporosis International* 16 (2005): 1412–1416.
- 7. R. J. Weiss, S. M. Montgomery, Z. Al Dabbagh, and K.-Å. Jansson, "National Data of 6409 Swedish Inpatients With Femoral Shaft Fractures: Stable Incidence Between 1998 and 2004," *Injury* 40, no. 3 (2009): 304–308.
- 8. S. B. Joglekar, E. M. Lindvall, and A. Martirosian, "Contemporary Management of Subtrochanteric Fractures," *Orthopedic Clinics* 46, no. 1 (2015): 21–35.
- 9. I. Garrison, G. Domingue, and M. W. Honeycutt, "Subtrochanteric Femur Fractures: Current Review of Management," *EFORT Open Rev* 6, no. 2 (2021): 145–151.
- 10. K. Matre, L. I. Havelin, J.-E. Gjertsen, T. Vinje, B. Espehaug, and J. M. Fevang, "Sliding Hip Screw Versus IM Nail in Reverse Oblique Trochanteric and Subtrochanteric Fractures. A Study of 2716 Patients in the Norwegian Hip Fracture Register," *Injury* 44, no. 6 (2013): 735–742.
- 11. J. O. Anglen, J. N. Weinstein, and Committee ABoOSR, "Nail or Plate Fixation of Intertrochanteric Hip Fractures: Changing Pattern of Practice: A Review of the American Board of Orthopaedic Surgery Database," *Journal of Bone and Joint Surgery-American Volume* 90, no. 4 (2008): 700–707.
- 12. E. H. Schemitsch, L. L. Nowak, A. P. Schulz, et al., "Intramedullary Nailing vs Sliding Hip Screw in Trochanteric Fracture Management: The INSITE Randomized Clinical Trial," *JAMA Network Open* 6, no. 6 (2023): e2317164-e.
- 13. E. Shane, D. Burr, P. R. Ebeling, et al., "Atypical Subtrochanteric and Diaphyseal Femoral Fractures: Report of a Task Force of the American Society for Bone and Mineral Research," *Journal of Bone and Mineral Research* 25, no. 11 (2010): 2267–2294.
- 14. H. Gao, J. Huang, Q. Wei, and C. He, "Advances in Animal Models for Studying Bone Fracture Healing," *Bioengineering* 10, no. 2 (2023): 201.
- 15. A. Bigham-Sadegh and A. Oryan, "Selection of Animal Models for Pre-Clinical Strategies in Evaluating the Fracture Healing, Bone Graft Substitutes and Bone Tissue Regeneration and Engineering," *Connective Tissue Research* 56, no. 3 (2015): 175–194.
- 16. I. Ohnishi, K. Oikawa, K. Tsuji, T. Ichikawa, and T. Kurokawa, "A Femoral Neck Fracture Model in Rabbits," *Journal of Biomechanics* 36, no. 3 (2003): 431–442.
- 17. T. Histing, P. Garcia, R. Matthys, et al., "An Internal Locking Plate to Study Intramembranous Bone Healing in a Mouse Femur Fracture Model," *Journal of Orthopaedic Research* 28, no. 3 (2010): 397–402.
- 18. R. M. Y. Wong, P. Y. Wong, C. Liu, et al., "3D Printing in Orthopaedic Surgery: A Scoping Review of Randomized Controlled Trials," *Bone & Joint Research* 10, no. 12 (2021): 807–819.
- 19. X.-H. Xie, X.-L. Wang, G. Zhang, et al., "Impaired Bone Healing in Rabbits With Steroid-Induced Osteonecrosis," *Journal of Bone & Joint Surgery British Volume* 93, no. 4 (2011): 558–565.
- 20. M. H. V. Choy, R. M. Y. Wong, M. C. Li, et al., "Can We Enhance Osteoporotic Metaphyseal Fracture Healing Through Enhancing Ultrastructural and Functional Changes of Osteocytes in Cortical Bone With Low-Magnitude High-Frequency Vibration?," *FASEB Journal* 34, no. 3 (2020): 4234–4252.
- 21. C. Sfeir, L. Ho, B. A. Doll, K. Azari, and J. O. Hollinger, "Fracture Repair," In *Bone Regeneration and Repair: Biology and Clinical Applications* (Springer, 2005), 21–44.
- 22. B. Beamer, C. Hettrich, and J. Lane, "Vascular Endothelial Growth Factor: An Essential Component of Angiogenesis and Fracture Healing," *HSS Journal* 6, no. 1 (2010): 85–94.

- 23. H. ElHawary, A. Baradaran, J. Abi-Rafeh, J. Vorstenbosch, L. Xu, and J. I. Efanov, "Bone Healing and Inflammation: Principles of Fracture and Repair," in *Semin Plast Surg*, vol. 35 (Thieme Medical Publishers, Inc., 2021), 198–203.
- 24. M. Klein, A. Stieger, D. Stenger, et al., "Comparison of Healing Process in Open Osteotomy Model and Open Fracture Model: Delayed Healing of Osteotomies After Intramedullary Screw Fixation," *Journal of Orthopaedic Research* 33, no. 7 (2015): 971–978.
- 25. C.-C. Hung, Y.-T. Li, Y.-C. Chou, et al., "Conventional Plate Fixation Method Versus Pre-Operative Virtual Simulation and Three-Dimensional Printing-Assisted Contoured Plate Fixation Method in the Treatment of Anterior Pelvic Ring Fracture," *International Orthopaedics* 43 (2019): 425–431.
- 26. J. Hayes and R. Richards, "The Use of Titanium and Stainless Steel in Fracture Fixation," *Expert Review of Medical Devices* 7, no. 6 (2010): 843–853.
- 27. W. Abd-Elaziem, M. A. Darwish, A. Hamada, and W. M. Daoush, "Titanium-Based Alloys and Composites for Orthopedic Implants Applications: A Comprehensive Review," *Materials & Design* 241 (2024): 112850.
- 28. R. Wong, U. Thormann, M. Choy, et al., "A Metaphyseal Fracture Rat Model for Mechanistic Studies of Osteoporotic Bone Healing," *European Cells & Materials* 37 (2019): 420–430.
- 29. B. B. Frade, L. D. da Cunha Muller, and D. C. Bonfim, "Establishing a Diaphyseal Femur Fracture Model in Mice," *Journal of Visualized Experiments* 190 (2022): e64766.

2734 Orthopaedic Surgery, 2025